2020 International Conference on Mathematical Neuroscience - Digital Edition (6th-7th of July 2020)

Dynamics of homogeneous and heterogeneous networks of Hodgkin-Huxley-type of models with bistability between bursting and silent states

Nataliya Stankevich, Aneta Koseska

National Research University High School of Economics, Nizhny Novgorod, Russia
Center of Advanced European Studies and Research, Bonn, Germany

6 of July 2020

Hodgkin-Huxley formalism

The Hodgkin – Huxley model is a mathematical model that describes the generation and distribution of action potentials in neurons. Similar models were subsequently created for other electrically excited cells: cardiac myocytes, pancreatic beta cells.

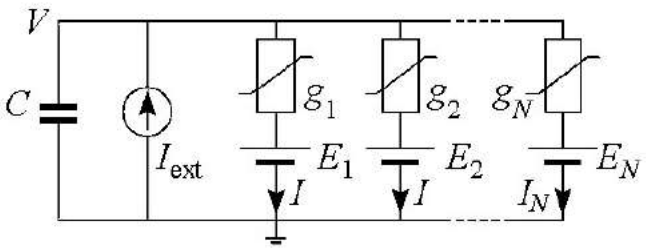

Equivalent scheme of neuron membrane

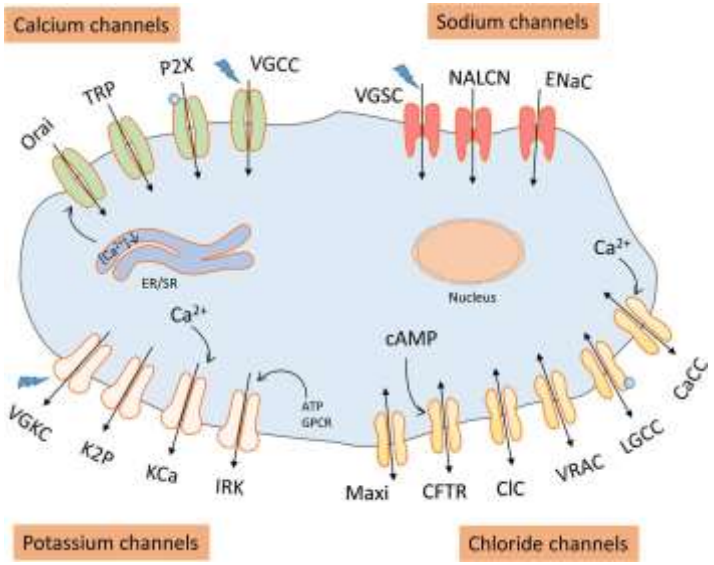

Hodgkin-Huxley model:

$$C\frac{dV}{dt} = I_{ext} - \sum_{j=1}^{N} I_j \qquad I_j = g_j(V - E_j)$$

$$C\frac{dV}{dt} = I_{ext} - \overline{g}_K n^4 (V - V_K) - \overline{g}_{Na} m^3 h (V - V_{Na}) - \overline{g}_L (V - V_L),$$

$$\frac{dx}{dt} = \alpha_x(V)(1 - x) - \beta_x(V)x.$$

Multistability is a ubiquitous Phenomenon

Multistability of oscillatory and silent regimes is a ubiquitous phenomenon exhibited by excitable systems such as neurons, cardiac cells, pancreatic beta-cells etc.

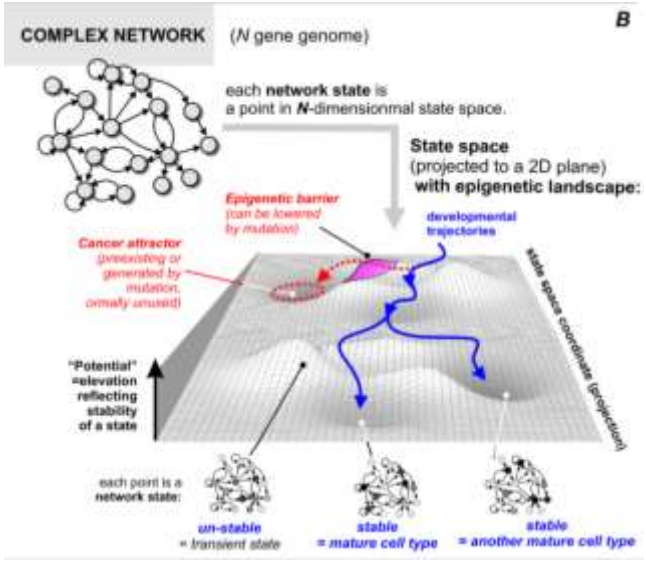

Published in final edited form as:
Semin Cell Dev Biol. 2009 September ; 20(7): 869–876. doi:10.1016/j.semcdb.2009.07.003.

Cancer attractors: A systems view of tumors from a gene network dynamics and developmental perspective

Sui Huang[*], **Ingemar Ernberg**[#], and **Stuart Kauffman**[*]
[*]Institute for Biocomplexity and Informatics, Biological Sciences Bldg, University of Calgary, Calgary AB, Canada

PNAS

Dynamics inside the cancer cell attractor reveal cell heterogeneity, limits of stability, and escape

Qin Li[a], Anders Wennborg[a], Erik Aurell[b], Erez Dekel[c], Jie-Zhi Zou[a], Yuting Xu[d], Sui Huang[e], and Ingemar Ernberg[a,1]

Pisarchik A.N., Feudel U., Control of multistability, Physics Reports, 2014, vol. 540, pp. 167-218.
Heyward, P., Ennis, M., Keller, A., & Shipley, M. T., Membrane bistability in olfactory bulb mitral cells, The Journal of Neuroscience, 2001, vol. 21. pp. 5311-5320.
Loewenstein, Y., Mahon, S., Chadderton, P., Kitamura, K., Sompolinsky, H., Yarom, Y., & Ha¨usser, M., Bistability of cerebellar Purkinje cells modulated by sensory stimulation, Nature neuroscience, 2005. vol. 8, pp. 202-211.
T. Malashchenko, A. Shilnikov, and G. Cymbalyuk, "Six types of multistability in a neuronal model based on slow calcium current," PloS One 518 6(7), e21782 (2011).

Hodgkin-Huxley-type of model with bursting

Sherman model

$$\tau\dot{V} = -I_{Ca}(V) - I_K(V,n) - I_S(V,S),$$
$$\tau\dot{n} = \sigma(n_\infty(V) - n),$$
$$\tau_S\dot{S} = S_\infty(V) - S.$$

$$I_{Ca}(V) = g_{Ca}m_\infty(V)(V - V_{Ca}),$$
$$I_K(V,n) = g_K n(V - V_K),$$
$$I_S(V,n) = g_S S(V - V_K),$$

$$\omega_\infty(V) = [1 + \exp\frac{V_\omega - V}{\theta_\omega}]^{-1}, \quad \omega = m,n,S$$

Table1. Parameters for original model

τ=	0.02sec	τS=	35sec	σ=	0.93
gCa=	3.6	gK=	10.0	gS=	4.0
VCa=	25.0mV	VK=	-75mV		
θm=	12.0mV	θn=	5.6mV	θs=	10.0mV
Vm=	-20.0mV	Vn=	-16.0mV	Vs=	-35mV

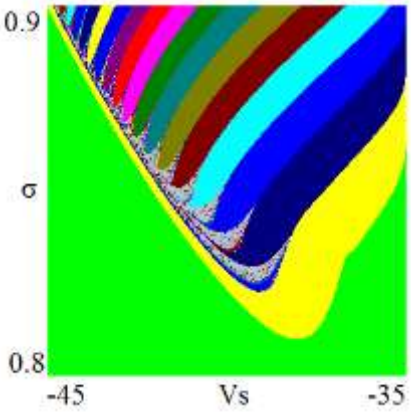

Chart of dynamical regimes

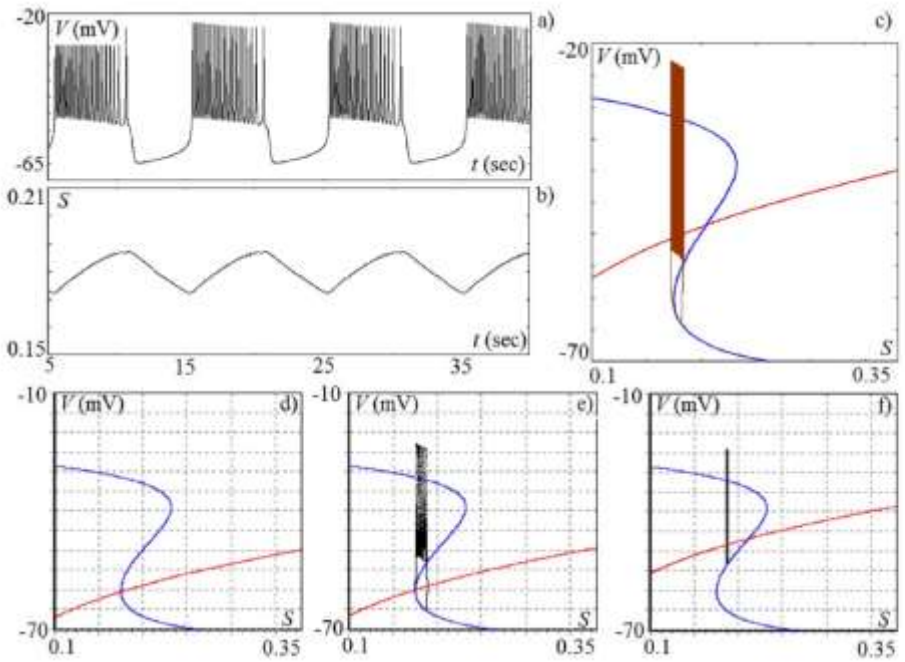

FIG. 1. Time series of the fast (a) and slow (b) variables; (c) fast (blue) and slow (red) manifolds together with a two-dimensional projection of phase portrait for the original Sherman model.[18] During the spiking phase, Ca^{2+}-ions flow into the cells and, during the silent phases, Ca^{2+}-ions are pumped out. The fast (spiking) dynamics is related to the flow of K^+-ions. (d) $V_S = -45$ mV; (e) $V_S = -44.7$ mV; and (f) $V_S = -33.7$ mV.

A. Sherman, J. Rinzel, and J. Keizer, "Emergence of organized bursting in 562clusters of pancreatic beta-cells by channel sharing," Biophys. J. 54(3), 563411–425 (1988).

Bistability between silent and bursting states

Stankevich N.V., Mosekilde E. Coexistence between silent and bursting states in a biophysical Hodgkin-Huxley-type of model // CHAOS. 2017. Vol. 27. Issue 11.

Modified model with new K^+ ion channel

EP (−49.084, 0.0027105, 0.19648)

$$\tau\dot{V} = -I_{Ca}(V) - I_K(V,n) - I_{K2}(V) - I_S(V,S),$$

$$\tau\dot{n} = \sigma(n_\infty(V) - n),$$

$$\tau_S\dot{S} = S_\infty(V) - S.$$

$$I_{K2}(V) = g_{K2}p_\infty(V)(V - V_K)$$

$$p_\infty(V) = [\exp\frac{V - V_p}{\theta_p} + \exp\frac{V_p - V}{\theta_p}]^{-1}$$

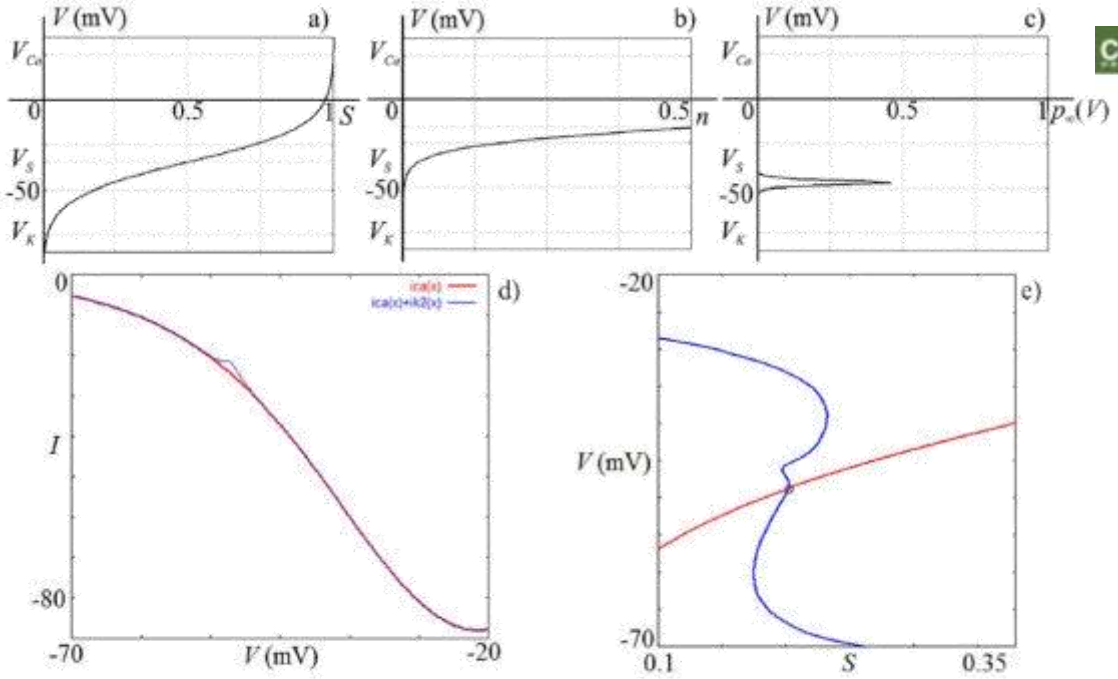

FIG. 2. Dependence of the membrane potential on the different ions: (a) calcium channel; (b) potassium channel; (c) probability function of new ion channel; (d) current of Ca^{2+} (2) (red) and sum of current Ca^{2+} (2) and current of new channel (6) (blue); (e) fast (blue) and slow (red) manifolds of the modified model (8). Supplementing parameters for the new ion channel: g_{K2}=0.14, θ_p=1 mV, and V_p=−46 mV.

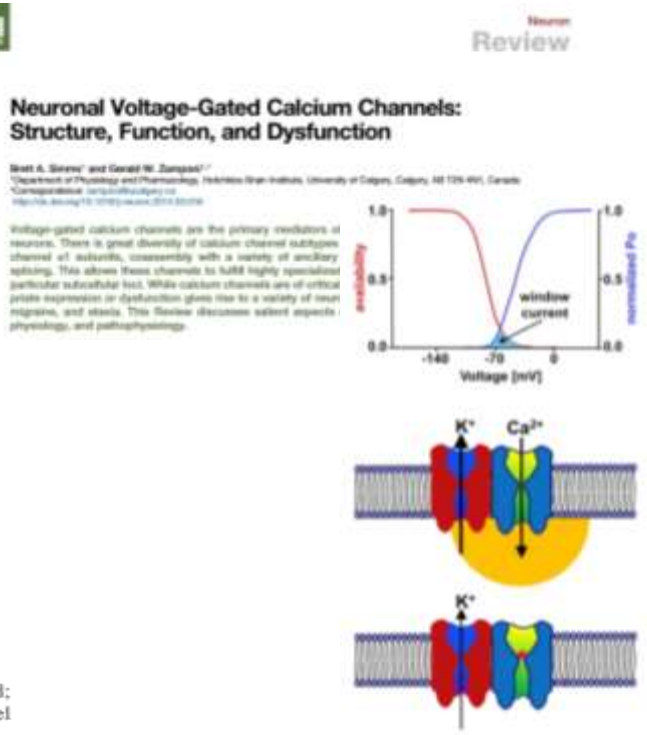

The simplest homogeneous networks:

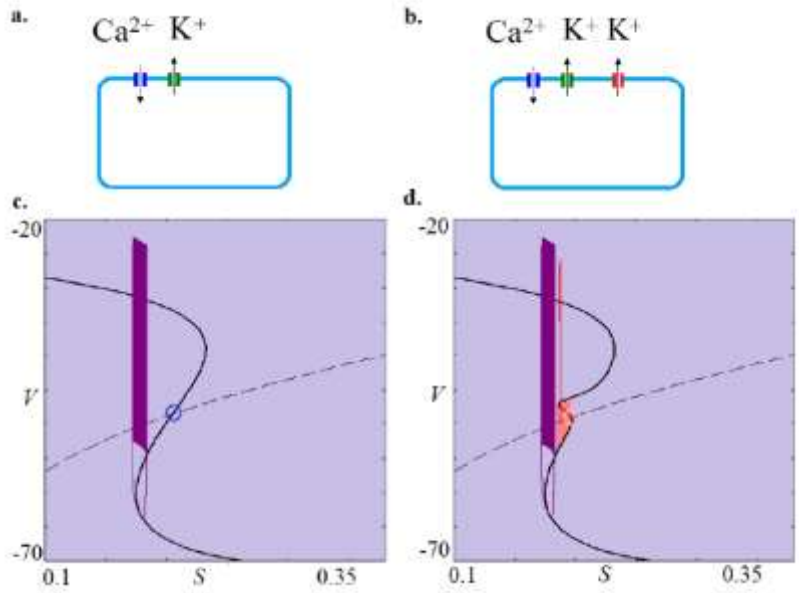

$$I_C(V^{(i)}) = \sum_{j \in \Gamma_i} g_{c,V}(V^{(i)} - V^{(j)}),$$

Typical dynamical behavior for coupled identical oscillators: multistability and chaos for small coupling and synchronization for larger coupling

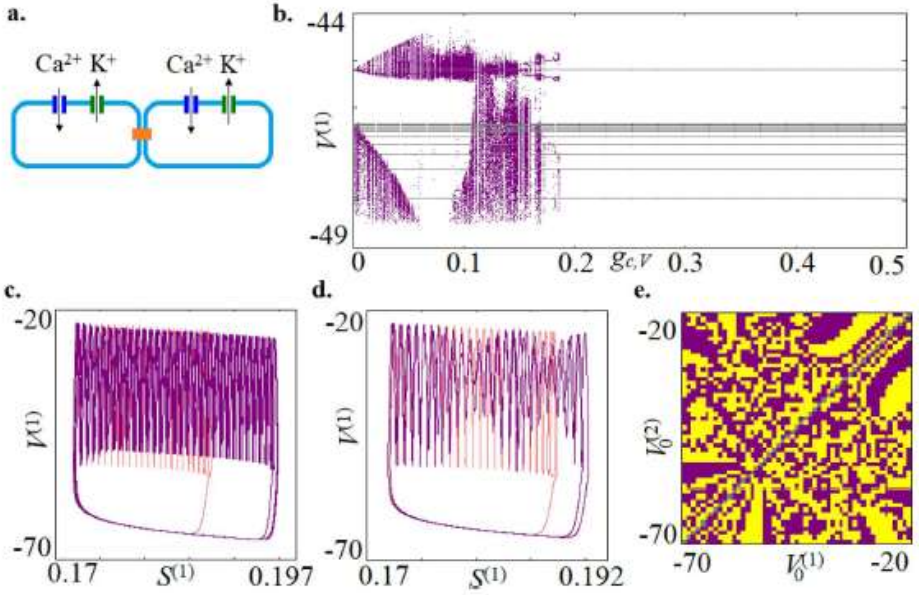

FIG. 2. Behavior of two coupled β-cells with bursting dynamics. (a) Schematic representation of the model. (b) Bifurcation trees estimated from Poincaré sections at the hypersurface $n^{(1)} = 0.003$ when $g_{c,V}$ is scanned in both directions (violet: forward, gray: backward). $k^{(i)} = 0, i = 1, 2$ and other parameters as in Fig. 1. Exemplary phase portraits depicting coexistence between synchronized bursting and (c) periodic or (d) aperiodic attractors are also shown for $g_{c,V} = 0.03$ and 0.15, respectively. (e) Estimated basins of attraction of the coexisting bursting attractors for $g_{c,V} = 0.15$ when starting from the following initial conditions: $n_0^{(1)} = 0.003$, $S_0^{(1)} = 0.188\,974\,7$, $n_0^{(2)} = 0.002\,503\,9$, $S_0^{(2)} = 0.188\,956\,6$.

The simplest homogeneous network with bistability

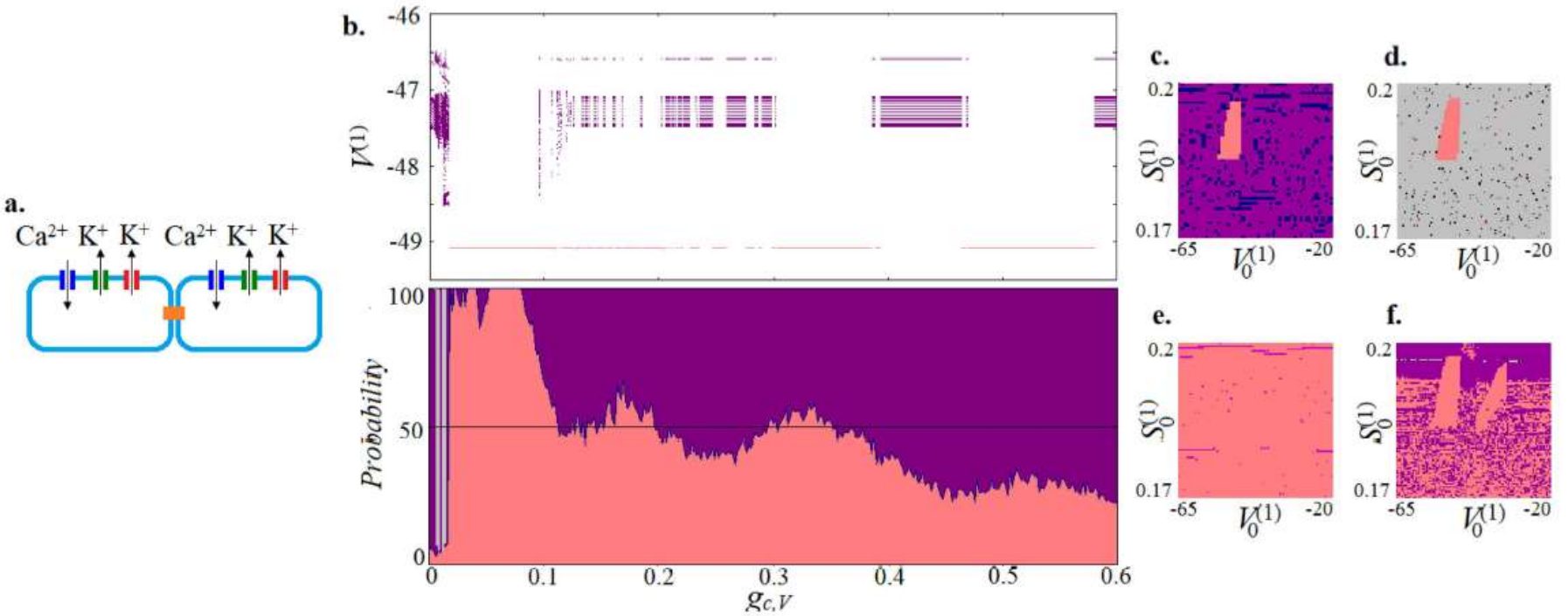

FIG. 3. Behavior of two coupled β-cells with dysfunctional potassium channels. (a) Schematic representation of the two-cell system. (b) (Top) Bifurcation tree estimated from Poincaré sections at the hypersurface and $n^{(1)} = 0.003$ constructed for fixed initial conditions: $V_0^{(1)} = -50.784$, $n_0^{(1)} = 0.0245$, $S_0^{(1)} = 0.1774$, $V_0^{(2)} = -49.084$, $n_0^{(2)} = 0.027\,105$, $S_0^{(2)} = 0.196\,48$, as well as (bottom) probability of the appearance of coexisting attractors in dependence on the coupling strength $g_{c,V}$. $k^{(i)} = 1$, $i = 1, 2$ and other parameters as in Fig. 1. Exemplary basins of coexisting attractors for various strength of coupling: (c) $g_{c,V} = 0.004$; (d) $g_{c,V} = 0.006\,63$; (e) $g_{c,V} = 0.02$; (f) $g_{c,V} = 0.12$. For (c)–(f), the initial conditions of the other variables were fixed in steady state $n_0^{(1)} = 0.027\,105$, $V_0^{(2)} = -49.084$, $n_0^{(2)} = 0.027\,105$, $S_0^{(2)} = 0.196\,48$. Gray: aperiodic dynamics; violet: bursting dynamics; red: steady state.

Larger homogeneous networks with bistability

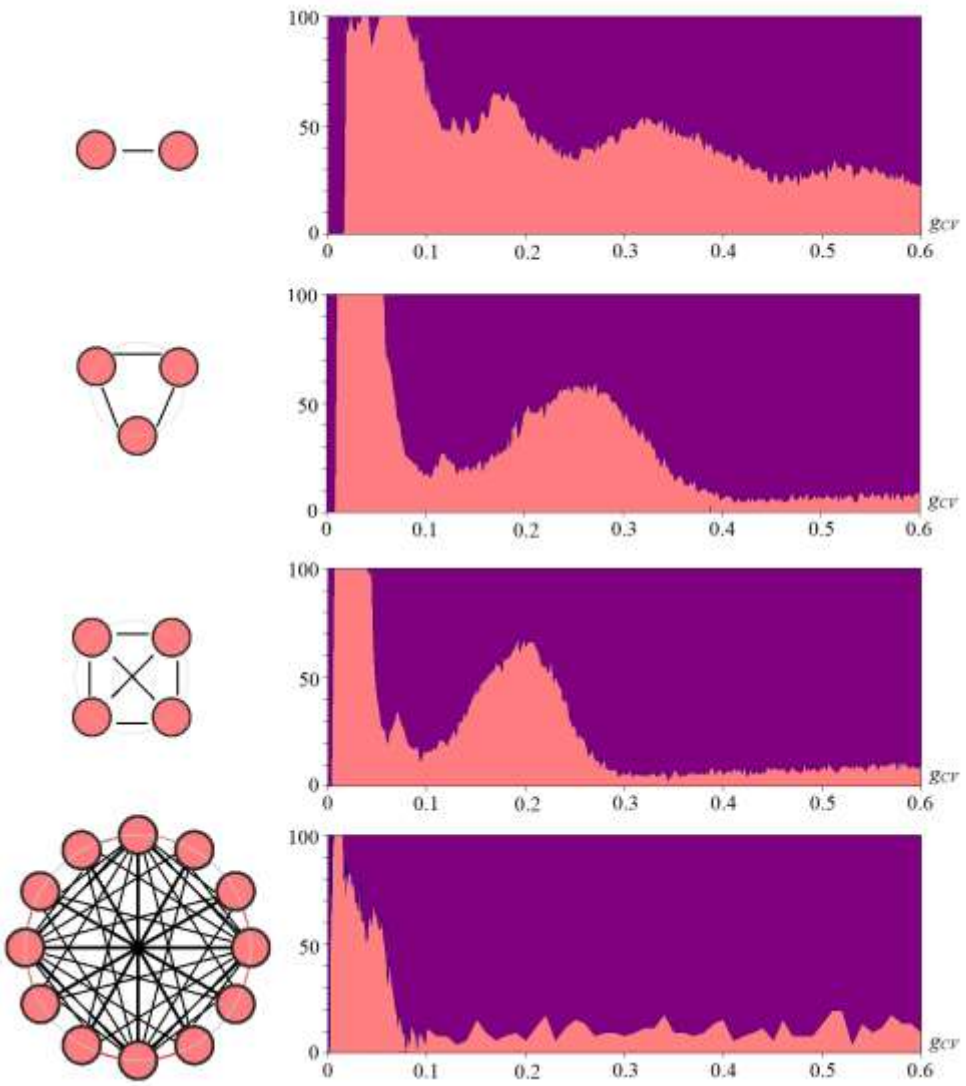

Fig. Behavior of network of coupled beta-cells with dysfunctional potassium channels. (a) Schematic representation of the network-cell system. (b) Probability of the appearance of coexisting attractors in dependence on the coupling strength gc,V . $k(i)$ = 1, i = 1, 2 and other parameters as in Fig. 1.

Dominance of silent dynamics for certain level of coupling strength

The simplest heterogeneous networks with bistability

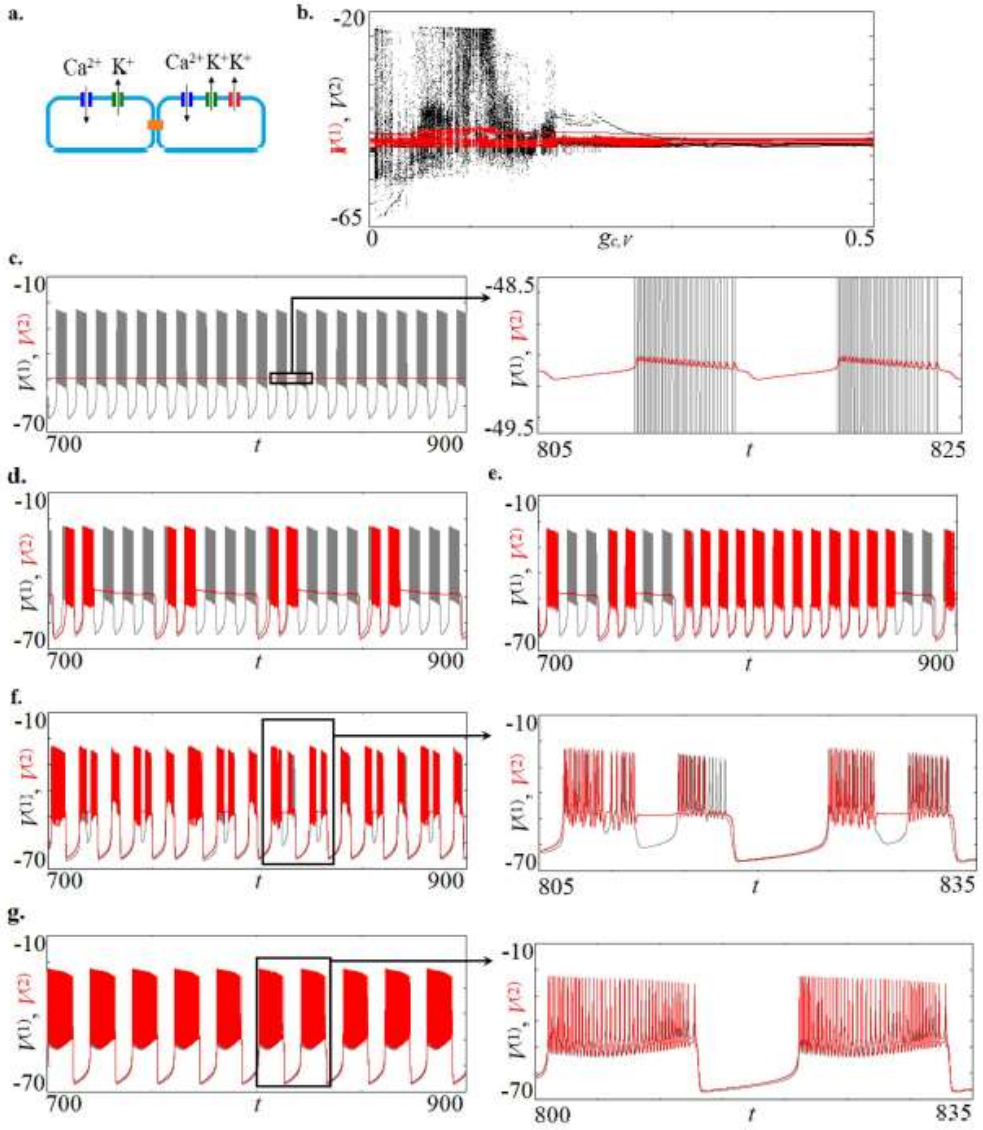

For minimal network silent state is not stabilized. Mix-mode dynamics is observed for small coupling strength. Synchronization for larger coupling.

FIG. 4. Behavior of a minimal mixed population model. (a) Schematic representation of minimal mixed population of two coupled cells (only one cell has channel dysregulation). (b) Bifurcation tree estimated from Poincaré sections at the hypersurface $n^{(1)} = 0.003$ when $g_{c,V}$ is scanned in both directions. $k^{(1)} = 0, k^{(2)} = 1$, and other parameters as in Fig. 1. Exemplary time series of characteristic dynamical regimes for (c) $g_{c,V} = 0.001$, (d) $g_{c,V} = 0.008$, (e) $g_{c,V} = 0.015$, (f) $g_{c,V} = 0.07$, (g) $g_{c,V} = 0.3$.

Larger heterogeneous networks with bistability

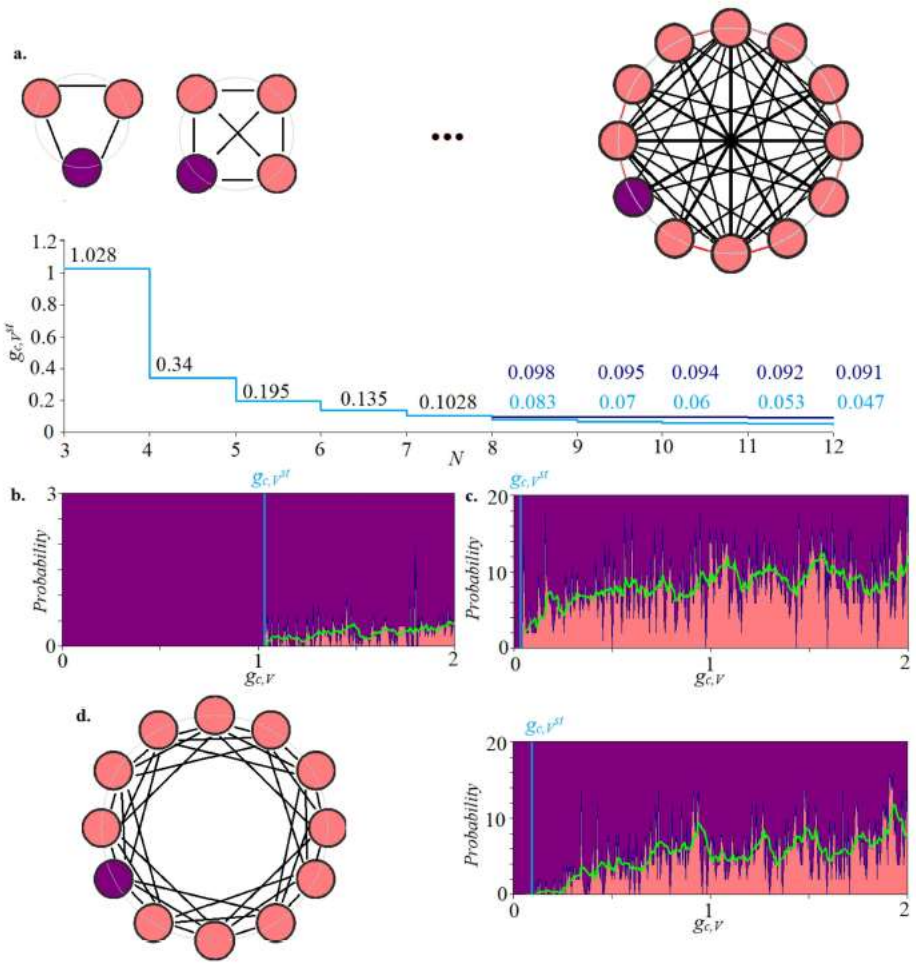

FIG. 5. Behavior of mixed β-cells population. (a) (Top) Schematic representation of globally coupled networks of increasing size, where only a single cell does not have a channel dysregulation (red color of node responds to $k^{(i)} = 1$, violet color to $k^{(i)} = 0$) and (bottom) a corresponding plots of coupling strength thresholds for steady state stabilization in dependence on the size of the population (N) for globally (light blue) and locally (dark blue) coupled cells. Schematic representation of locally coupled population in Fig. 5(d), left. Probability of the appearance of coexisting attractors in dependence on the coupling strength for the minimal population (b) of $N = 3$ coupled cells, as well as for (c) $N = 12$ globally or (d) locally coupled cells. Other parameters as in Fig. 1. $g^{st}_{c,V}$ - $g_{c,V}$, threshold for which the steady state is stabilized.

Stabilization of equilibrium is possible for larger networks , when number of oscillators with bistability more then N/2, N is size of network.
Effect for globally and locally coupled network is the same.

Conclusion

Homogenous networks with bistability demonstrates dominance of silent dynamics for certain level of coupling.

In heterogeneous networks stabilization of equilibrium is possible, when number of oscillators with bistability more then 50% in network.

Stabilized silent state in heterogeneous networks doesn't dominate, possibility to obtain such kind of behavior is less the 20%

Effect for globally and locally coupled networks is the same.